

A Mutation in *VEGFC*, a Ligand for VEGFR3, is Associated with Autosomal Dominant Milroy-like Primary Lymphedema

Running title: Mutation in *VEGFC* Causes Primary Lymphedema

Kristiana Gordon*, Dörte Schulte*, Glen Brice, Michael A Simpson, Guy Roukens, Andreas van Impel, Fiona Connell, Kamini Kalidas, Steve Jeffery, Peter S Mortimer, Sahar Mansour, Stefan Schulte-Merker, Pia Ostergaard

KG, PSM: Department of Clinical Sciences, St George's University of London, London SW17 0RE, UK

DS, GR, AvI, SSM: Hubrecht Institute, KNAW – UMC Utrecht, 3584 CT Utrecht, Netherlands

GB, SM: SW Thames Regional Genetics Service, St. George's University of London, London SW17 0RE, UK

MAS: Division of Genetics and Molecular Medicine, King's College London School of Medicine, Guy's Hospital, London SE1 9RT, UK

FC: Clinical Genetics, Guy's and St Thomas' NHS Foundation Trust, Guy's Hospital, London SE1 9RT, UK

KK, SJ, PO: Human Genetics Research Centre, Biomedical Sciences, St. George's University London, London SW17 0RE, UK

SSM: EZO, Wageningen University, Netherlands

*equal contribution

Corresponding author: Pia Ostergaard

Email: p.ostergaard@sgul.ac.uk

Telephone: +44 (0)2087250192

Word count: 2496

Subject codes: [109], [130], [139], [147]

Abstract

Rationale: Mutations in *VEGFR3 (FLT4)* cause Milroy Disease (MD), an autosomal dominant condition that presents with congenital lymphedema. Mutations in *VEGFR3* are identified in only 70% of patients with classic MD, suggesting genetic heterogeneity.

Objective: To investigate the underlying cause in patients with clinical signs resembling MD in whom sequencing of the coding region of *VEGFR3* did not reveal any pathogenic variation.

Methods and Results: Exome sequencing of five such patients was performed and a novel frameshift variant, c.571_572insTT in *VEGFC*, a ligand for VEGFR3, was identified in one proband. The variant co-segregated with the affected status in the family. An assay to assess the biological function of VEGFC activity *in vivo*, by expressing human VEGFC in the zebrafish floorplate was established. Forced expression of wildtype human VEGFC in the floorplate of zebrafish embryos leads to excessive sprouting in neighbouring vessels. However, when overexpressing the human c.571_572insTT variant in the floorplate, no sprouting of vessels was observed, indicating that the base changes have a marked effect on the activity of VEGFC.

Conclusions: We propose that the mutation in *VEGFC* is causative for the MD-like phenotype seen in this family. This is the first time a mutation in one of the ligands of VEGFR3 has been reported to cause primary lymphedema.

Key Words: *VEGFC*, Milroy Disease, Primary Lymphedema, *VEGFR3*, *FLT4*

Non-standard Abbreviations and Acronyms	
PL	Primary lymphedema
MD	Milroy Disease
VEGFC	Vascular endothelial growth factor – C
VEGFR3/FLT4	Vascular endothelial growth factor receptor -3
hVEGFC	Human wildtype VEGFC
hVEGFCinsTT	Human mutant VEGFC
YFP+	Yellow fluorescent protein positive

Primary lymphedema (PL) is clinically and genetically heterogeneous.¹ PL is caused by anatomical or functional defects in the lymphatic system, leading to chronic swelling of one or more body parts. To date, mutations in seven genes, *CCBE1* (MIM 235510), *FOXC2* (MIM 153400), *GATA2* (MIM 614038), *GJC2* (MIM 613480), *KIF11* (MIM 152950), *SOX18* (MIM 607823), and *VEGFR3* (MIM 153100) have been identified as causative for disorders in which PL is a major feature. Still, there are a substantial number of PL patients where the underlying cause has yet to be identified.

Milroy Disease (MD) is an autosomal dominant, congenital form of PL with reduced penetrance. The edema is usually painless and chronic, presenting most often at birth, bilaterally, and are confined to the dorsum of the foot.² Swellings can extend further up the lower limb and great variability of expression has been reported. Mutations in *VEGFR3* (Vascular Endothelial Growth Factor Receptor 3) are known to be causative for about 70% of MD³ cases and these have recently been summarised.⁴ Despite several candidate gene screening efforts, no other genes have been associated with MD to date.

Methods

An expanded Methods section including a detailed clinical description of the whole family is available in the Online Supplement.

Results

We present a multi-generational pedigree in which MD-like lymphedema segregates in a pattern consistent with autosomal dominant inheritance (Figure 1A). The index patient (Patient II:4) is a male that on examination revealed moderate lymphedema affecting the left below-knee region, with less severe changes in the right below-knee region (Figure 1B). His mother (Patient I:2) had suffered with bilateral below-knee lymphedema since childhood (Figure 1C). The proband's sister (Patient II:3) presented with congenital lymphedema of both feet and ankles and had prominent veins around the ankles and dorsum of the feet (Figure 1D). Patient II:3 had a son (Patient III:2) with congenital lymphedema and prominent veins of both feet and ankles (Figure 1D). His swelling spontaneously improved in the third year of life. The affected family members show variable clinical signs, which is common in MD² and are described in greater detail in the Online Supplement.

While the index patient's presentation was suggestive of MD, he was found to be negative for *VEGFR3* mutations. Whole exome sequencing was performed and we identified one heterozygous frameshift variant (c.571_572insTT; p.Pro191Leufs*10) in *VEGFC* (Figure 2A). The change is predicted to be disease-causing, and co-segregated with the disease status in the rest of the family upon Sanger sequencing (LOD score 2.1).

The affected family members underwent lymphoscintigraphy which showed reduced uptake with tortuous lymphatic tracts and evidence of re-routing (Figure 1F). This contrasts with the

lymphoscintigrams seen in MD patients with proven mutations in *VEGFR3*, which show no uptake within the main lymphatic tracts after 2 hours, suggestive of initial lymphatic vessel dysfunction (Figure 1G).

VEGFC codes for one of the ligands of the tyrosine kinase receptor *VEGFR3*. The c.571_572insTT mutation lies within exon 4, encoding part of the VEGF homology domain of *VEGFC*, leading to a predicted frameshift from codon 191 and a stop codon ten amino acids further downstream (Figure 2B). We analysed stability and secretion of the c.571_572insTT variant (*VEGFCinsTT*) by Western blotting of lysates and supernatants of 293T cells transiently transfected with wildtype human *VEGFC* (*hVEGFC*) and the *hVEGFCinsTT* variant. In *hVEGFC* transfected cell lysates and supernatants, we detected bands corresponding in size to the differentially processed isoforms of *VEGFC* (58kD, 31kD, 21kD and 15kD)(Figure 2C). In lysates of cells transfected with the *hVEGFCinsTT* variant, we detected a band of approximately 22kD, the predicted molecular weight of the variant, but did not detect any protein in the supernatant (Figure 2C). Thus, while *VEGFCinsTT* encodes a stable protein in cell lysates, secretion of this mutant variant is strongly impaired as compared to wildtype *VEGFC*.

To analyze the activity of the c.571_572insTT variant *in vivo*, we established an assay in zebrafish by over-expressing *hVEGFC* and *hVEGFCinsTT* in the floorplate while monitoring expression by an IRES tagRFP cassette. Zebrafish *Vegfc* shares 57% identity with human *VEGFC*, and in zebrafish, *Vegfc* signalling via *Vegfr3* is required for venous angiogenic sprouting⁵ and the development of the lymphatic system.⁶ Simultaneous over-expression of *hVEGFC* and tagRFP in the floorplate of zebrafish embryos led to excessive vessel sprouting at 56hpf (Figure 3D), while overexpression of tagRFP alone had no effect on vessel growth (Figure 3C). *hVEGFC* overexpression promoted hypersprouting of venous and lymphatic vessels, but not of arterial vessels (Online Figure II). We used this model for testing pathogenicity of the c.571_572insTT mutation *in vivo*. In contrast to the expression of *hVEGFC*, expression of *hVEGFCinsTT* and tagRFP in the floorplate had no detectable effect (Figure 3E), indicating that the mutation significantly reduces, or possibly completely abolishes, the biological activity of the protein.

We also considered the possibility of the mutation resulting in a truncated protein with dominant negative properties. However, expressing the c.571_572insTT allele in the zebrafish floorplate assay did not interfere with normal vasculogenesis or angiogenesis, rendering the possibility of a dominant negative effect unlikely. Furthermore, we co-overexpressed *hVEGFC* and *hVEGFCinsTT* in the zebrafish floorplate, monitoring levels of *hVEGFC* and *hVEGFCinsTT* using IRES tagRFP and IRES mTurquoise cassettes, respectively. Co-overexpression led to hypersprouting at a similar level to embryos expressing only *hVEGFC* in the floorplate (Figure 4). Note that the two transgenes were expressed in the

same cells (Online Figure III). We conclude that the VEGFC insTT variant does not have dominant negative activity, but most likely leads to a haplo-insufficient phenotype.

Discussion

VEGFC belongs to the family of vascular endothelial growth factors (VEGFs), which act as ligands for transmembrane tyrosine kinase receptors of the VEGF-receptor family. The c.571_572insTT variant reported here encodes a truncating mutation predicted to be pathogenic using protein structure prediction and a functional assay. *In vitro* data suggest that the protein is indeed truncated, stable, but does not get secreted efficiently. Hence, in patients this would result in a presumed reduction of VEGFC protein by 50% which leads to mild edema formation. Interestingly, haplo-insufficient *Vegfc* mice and *Chy3* mice (hemizygous for *Vegfc*) survive to adulthood with paw edema and a hypoplastic dermal lymphatic network^{7,8} and the two mouse models are good representatives of the human phenotype. As we have found no evidence for a dominant negative effect of the protein variant, the human patients are likely to present haplo-insufficient scenarios.

To date, only one *VEGFC* mutation positive patient, and six affected family members have been identified. Screening of a small selection (n=16) of patients with a similar phenotype did not identify additional mutations in the ligand. Other unknown ligands and ligand-independent signalling via VEGFR3⁹ may explain why mutations in *VEGFC* are only responsible for a small fraction of MD-like cases. It is also possible that proband and his family is genetically protected and can compensate for the presumed loss of VEGFC activity by other factors. Further studies are required to fully elucidate this.

In conclusion, we have identified a *VEGFC* mutation that causes a Milroy-like primary lymphedema. Our findings demonstrate that mutations in VEGFC can cause a phenotype similar to that found in patients with mutations in the VEGFC receptor, VEGFR3. We propose that *VEGFC*-screening should be considered in patients presenting with a Milroy-like phenotype but no identifiable *VEGFR3* mutation, particularly if the lymphoscintigram demonstrates poor uptake with tortuous lymphatics and re-routing. This is the first report in the literature of a human phenotype associated with a *VEGFC* mutation.

Sources of Funding

KG and PO: British Heart Foundation (FS/11/40/28739 and PG/10/58/28477); SSM: KNAW; DS and AvI: MC IEP awards; GR: VENI grant. Supported by the Department of Health via the NIHR comprehensive BRC award to GSTT NHS Foundation Trust in partnership with KCL and KCH NHS Foundation Trust. Supported by the Biomics Centre, St. George's University of London.

Disclosures

None.

Figure 1. Pedigree and clinical manifestations. (A) Index case is indicated by an arrow. Note high degree of variability of clinical signs within the family. (B) Index patient (II:4) demonstrating swelling of the left below-knee region with clear skin changes (e.g. hyperkeratosis). Less severe swellings of right foot and ankle are present. (C) Patient I:2 demonstrating bilateral lower limb lymphedema extending up to the knee. Notice the venous flares on her feet and shin. (D) Patient II:3 and her son (III:2) demonstrating lower limb lymphedema and prominent veins (arrow) on dorsum of feet. (E-G) Anterior view of lower limb lymphoscintigraphy; (E) healthy control, (F) patient II:4 demonstrating re-routing of tracer around the feet, ankles and lower legs. Some filling of the main lymphatic tracts is seen in the region of the knees with faint uptake in these main tracts to the groin, with less uptake in left groin in keeping with asymmetry of edema. (G) Typical Milroy Disease with no visible main-tract filling nor re-routing (functional aplasia).

Figure 2: c.571_572insTT VEGFC protein is not secreted efficiently. (A) Sequencing of the index patient revealed a TT insertion at base position 571 leading to a premature stop at amino acid 200. (B) Schematic representation of predicted wildtype and mutant proteins. (C) Western Blot analysis of 293T cells transiently transfected with human VEGFC or the VEGFCinsTT variant. Differentially processed isoforms (58kD, 31kD, 21kD and 15kD) can be detected in cell lysate and supernatant of cells transfected with VEGFC cDNA. A 22kD and a smaller band can be detected in lysates of cells transfected with the VEGFCinsTT variant cDNA, but not in the supernatant of these cells.

Figure 3: 571_572insTT mutation in human VEGFC abolishes the effect of ectopic expression on neighbouring vessels. (A) Overview of the endothelial network (blue) and the spatial distribution of both the endogenous zebrafish vegfc (EN vegfc; green) and the human VEGFC expressed in the floorplate (FE, red). DLAV: dorsal longitudinal anastomotic vessel, ISV: intersegmental vessel, PL: parachordal lymphangioblast, DA: dorsal aorta, PCV: cardinal vein. (B-E) Analysis of hVEGFC overexpression in the floorplate using the transgenic line TG(flt4:YFP) at 56hpf. (B) Non-injected control; (C) tagRFP only. (D) Forced expression of hVEGFC in the floorplate led to excessive vessel sprouting; (E) over-expression of hVEGFCinsTT in the floorplate resulted in embryos indistinguishable from control embryos. (F-G) The black and white threshold images (inserts in B-E) exhibit comparable expression of RFP and were used to quantify vessel sprouting and the YFP+ area. (F) Quantification of YFP+ area, (G) number of branch points per magnified areas.

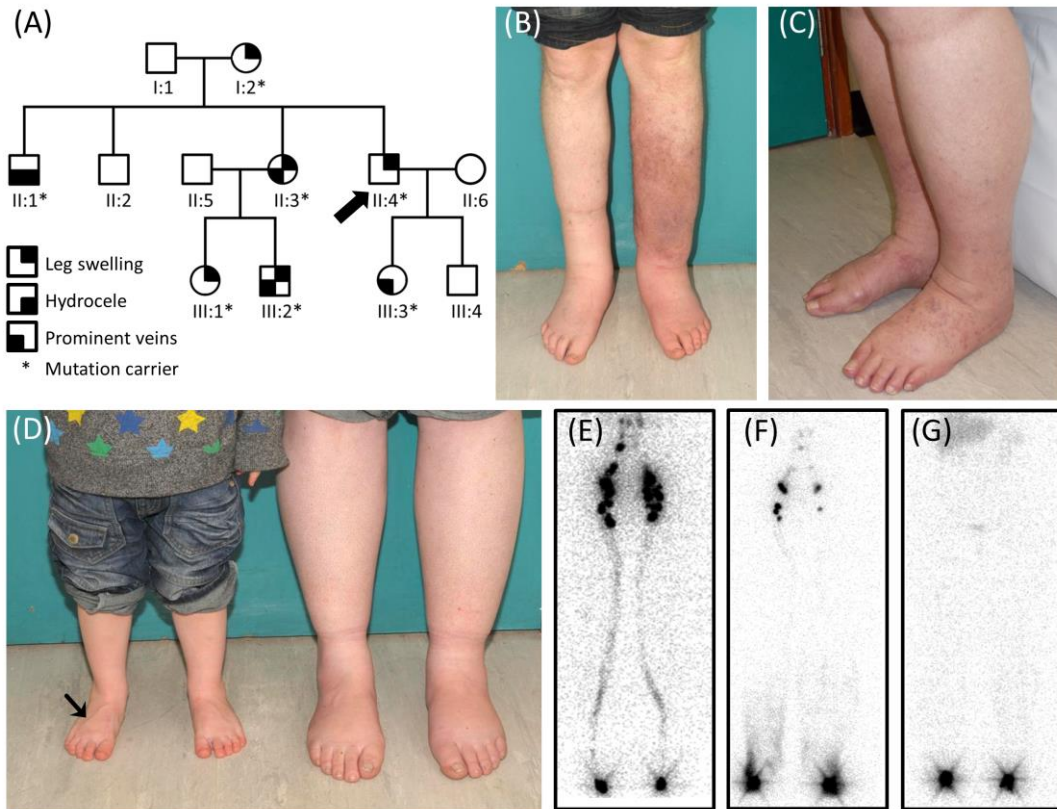
Figure 4. The VEGFCinsTT variant does not have dominant negative activity. (A-B) Analysis of co-overexpression of hVEGFC and hVEGFCinsTT in the floorplate using the transgenic line TG(flt4:YFP) at 56hpf. (A) Forced expression of hVEGFC in the floorplate led to excessive vessel sprouting comparable to (B) co-over-expression of hVEGFCinsTT and hVEGFC in the

floorplate. **(C)** Quantification of YFP+ area and **(D)** number of branch points in the black and white threshold images (inserts in **A-B**).

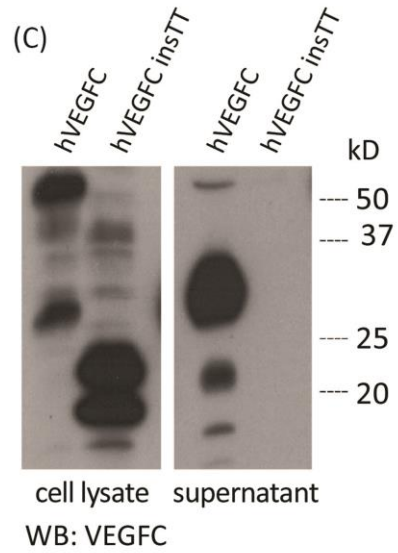
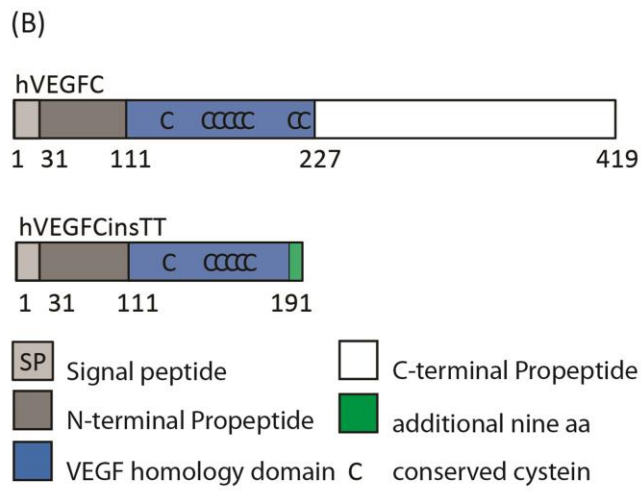
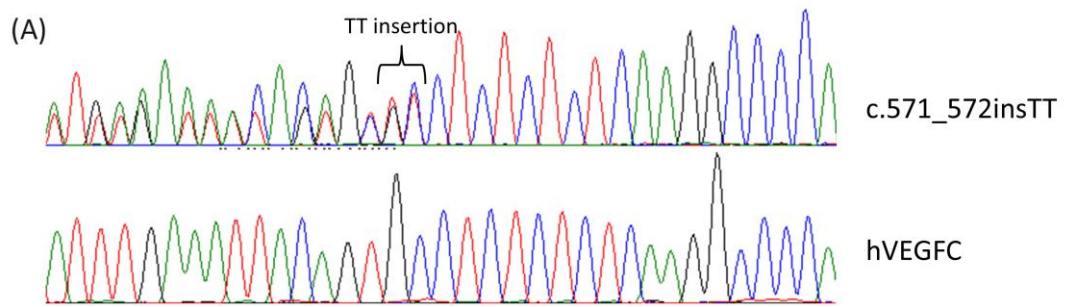
References

1. Connell F, Brice G, Jeffery S, Keeley V, Mortimer P, Mansour S. A new classification system for primary lymphatic dysplasias based on phenotype. *Clinical Genetics*. 2010;77:438-452
2. Brice G, Child AH, Evans A, Bell R, Mansour S, Burnand K, Sarfarazi M, Jeffery S, Mortimer P. Milroy disease and the vegfr-3 mutation phenotype. *Journal of Medical Genetics*. 2005;42:98-102
3. Connell FC, Ostergaard P, Carver C, Brice G, Williams N, Mansour S, Mortimer PS, Jeffery S, Lymphoedema C. Analysis of the coding regions of vegfr3 and vegfc in milroy disease and other primary lymphoedemas. *Human Genetics*. 2009;124:625-631
4. Gordon K, Spiden SL, Connell FC, Brice G, Cottrell S, Short J, Taylor R, Jeffery S, Mortimer PS, Mansour S, Ostergaard P. Flt4/vegfr3 and milroy disease: Novel mutations, a review of published variants and database update. *Human mutation*. 2013;34:23-31
5. Hogan BM, Bos FL, Bussmann J, Witte M, Chi NC, Duckers HJ, Schulte-Merker S. Ccbe1 is required for embryonic lymphangiogenesis and venous sprouting. *Nature Genetics*. 2009;41:396-398
6. Kuchler AM, Gjini E, Peterson-Maduro J, Cancilla B, Wolburg H, Schulte-Merker S. Development of the zebrafish lymphatic system requires vegfc signaling. *Current Biology*. 2006;16:1244-1248
7. Karkkainen MJ, Haiko P, Sainio K, Partanen J, Taipale J, Petrova TV, Jeltsch M, Jackson DG, Talikka M, Rauvala H, Betsholtz C, Alitalo K. Vascular endothelial growth factor c is required for sprouting of the first lymphatic vessels from embryonic veins. *Nature Immunology*. 2004;5:74-80
8. Dellinger MT, Hunter RJ, Bernas MJ, Witte MH, Erickson RP. Chy-3 mice are vegfc haploinsufficient and exhibit defective dermal superficial to deep lymphatic transition and dermal lymphatic hypoplasia. *Developmental Dynamics*. 2007;236:2346-2355
9. Galvagni F, Pennacchini S, Salameh A, Rocchigiani M, Neri F, Orlandini M, Petraglia F, Gotta S, Sardone GL, Matteucci G, Terstappen GC, Oliviero S. Endothelial cell adhesion to the extracellular matrix induces c-src-dependent vegfr-3 phosphorylation without the activation of the receptor intrinsic kinase activity. *Circulation Research*. 2010;106:1839-U1125

Mutation in *VEGFC* Causes Primary Lymphedema

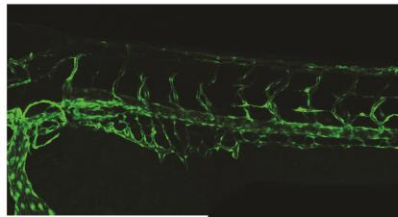
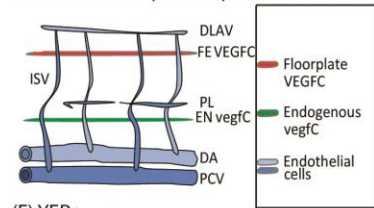


Mutation in VEGFC Causes Primary Lymphedema

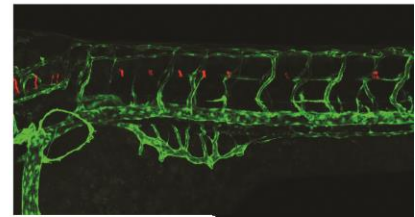


Mutation in *VEGFC* Causes Primary Lymphedema

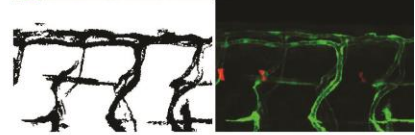
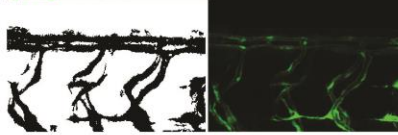
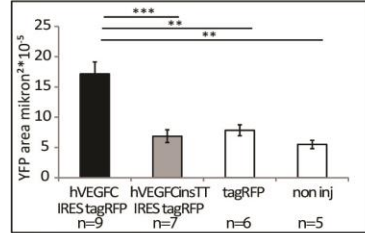
(A) Forced floor plate expression of VEGFC (B) non injected control



(C) tagRFP

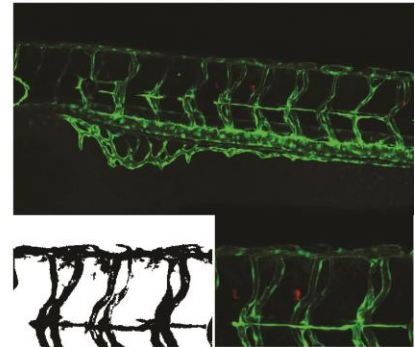
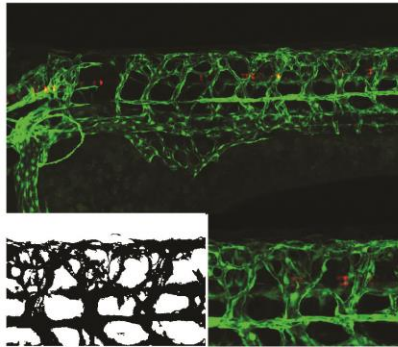


(F) YFP+ area

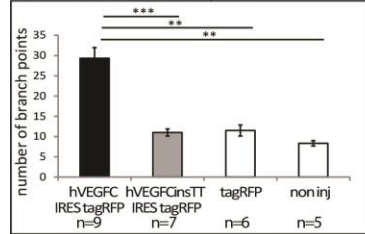


(D) hVEGFC IRES tagRFP

(E) hVEGFCinsTT IRES tagRFP



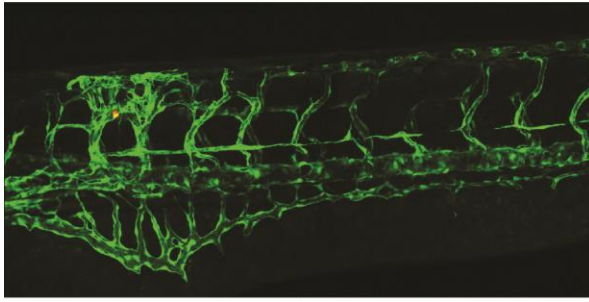
(G) Number of branch points



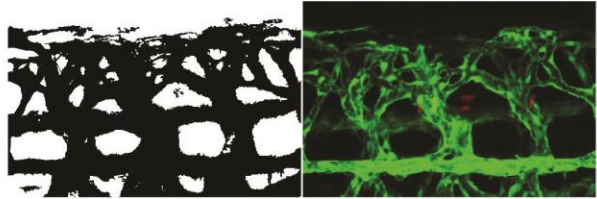
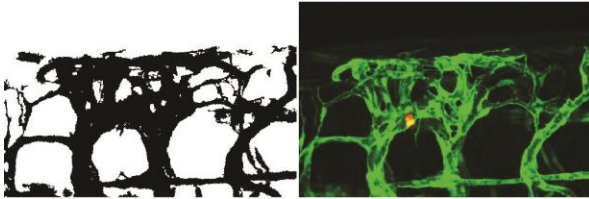
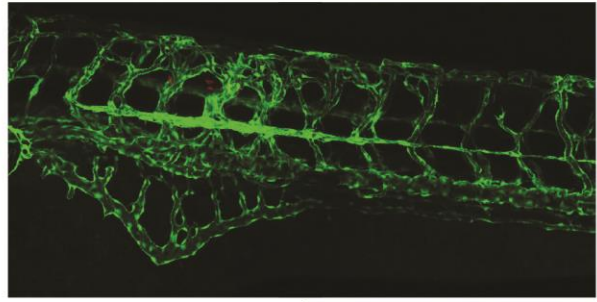
* = P<0.05; ** = P<0.01; *** = P<0.001.

Mutation in *VEGFC* Causes Primary Lymphedema

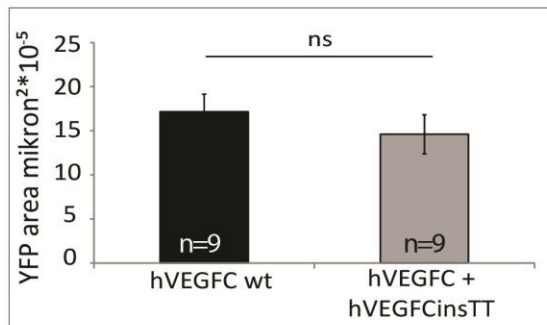
(A) hVEGFC IRES tagRFP



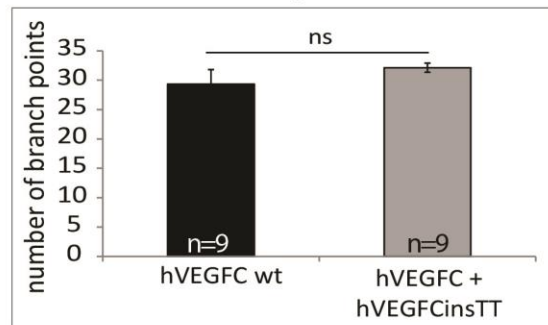
(B) hVEGFC IRES tagRFP + hVEGFCinsTT IRES mTurquoise



(C) YFP+ area



(D) Number of branch points



ns: not significant

A Mutation in *VEGFC*, a Ligand for VEGFR3, is Associated with Autosomal Dominant Milroy-like Primary Lymphedema

Kristiana Gordon*, Dörte Schulte*, Glen Brice, Michael A Simpson, Guy Roukens, Andreas van Impel, Fiona Connell, Kamini Kalidas, Steve Jeffery, Peter S Mortimer, Sahar Mansour, Stefan Schulte-Merker, Pia Ostergaard

Supplement Material and Methods

Family Recruitment

Proband and family were ascertained through the Primary Lymphedema (PL) Clinic at St George's Hospital, London, UK. The study obtained ethical approval (South West London Research Ethics Committee – REC Ref: 05/Q0803/257) and written informed consent was obtained from all participants (n=12). Samples for subsequent *VEGFC* screening were also obtained through the same clinic.

Case Study

The index patient (Patient II:4 in Figure 1A) was a male aged 32 years, the eldest child of unrelated Caucasian parents. He presented with congenital lymphedema of the left foot and ankle. During childhood he developed swelling of the right foot and ankle, but to a lesser degree. He had no hydroceles and no past medical history of note. Examination revealed moderate lymphedema affecting the left below-knee region (Figure 1B). Skin changes included hyperkeratosis, papillomatosis and fibrosis. Less severe changes were present in the right below-knee region. He had a history of a few episodes of left leg cellulitis.

Lymphoscintigraphy examination, imaged 2 hr after injection of radioactive isotope [technetium 99] into the webspaces between the toes, revealed impaired lymphatic drainage in both lower limbs with only 4.8% of tracer activity reaching the right groin and 0.8% reaching the left groin after two hours (less than 8% of tracer in the inguinal lymph nodes at two hours is considered abnormal). Images showed re-routing of tracer around the foot, ankle and lower legs. Some filling of the main lymphatic tracts is subsequently seen in the region of the knees with faint uptake in these main tracts to the groin. There was a reduction in uptake of tracer within the groin lymph nodes, the left side affected more than the right, in keeping with the severity of his lymphedema (Figure 1F). Scan appearances were similar but not typical of those seen in patients with Milroy disease (Figure 1G) and very different from a healthy control (Figure 1E). The index patient had two children, a son

Mutation in *VEGFC* Causes Primary Lymphedema

aged six years (Patient III:4) and a daughter aged five years (Patient III:3). The boy had no evidence of lymphedema or hydroceles. The girl had no evidence of lymphedema but had prominent, large calibre veins in her lower legs and on the dorsum of her feet.

The proband's sister (Patient II:3), aged 28, presented with congenital lymphedema of both feet and ankles. The swelling spontaneously improved without medical intervention during childhood but deteriorated again in adolescence. Examination revealed bilateral, below knee lymphedema with prominent veins around the ankles and dorsum of the feet (Figure 1D). Lymphoscintigraphy revealed tortuous tracts in the right lower limb but with rapid uptake of tracer to the right groin after 15 minutes. A normal amount (19%) of tracer was detected in the right inguinal lymph nodes after two hours. The left lower limb had an abnormal pattern similar to that of Patient II:4, with re-routing around the left ankle and only 2.3% of tracer reaching the left inguinal lymph nodes after two hours. Patient II:3 had two children, a boy aged three (Patient III:2) and a daughter aged six months (Patient III:1). Her son presented with congenital lymphedema and prominent veins of both feet and ankles. He had no other health problems, notably no hydroceles. His swelling spontaneously improved in the third year of life. The daughter had no evidence of lymphedema at birth, but developed lymphedema of feet and ankles at the age of six months.

The proband had an unaffected brother aged 23 years (Patient II:2). His youngest brother, aged 18 years (Patient II:1) had no evidence of lymphedema, but he did have prominent veins of the ankles and feet and bilateral hydroceles (age of onset: 12y) that were refractory to surgical correction. Lymphoscintigraphy revealed abnormal tortuous lymphatic tracts of both lower limbs. 10% of tracer reached the right inguinal lymph nodes and 11% reached the left at two hours. Despite these normal levels within the inguinal nodes, the patient has impaired lymphatic drainage as a high level of tracer (83%) remained within the right foot after two hours, confirming poor clearance by the lymphatic system.

The proband's father (Patient I:1) had no clinical signs of lymphedema or hydroceles. The mother (Patient I:2) had suffered with bilateral below-knee lymphedema since childhood (Figure 1C), but had not sought medical advice on this matter. She was uncertain whether the onset was congenital or within the first few years of life. Although she had clinical signs of venous hypertension (i.e. venous flares and telangiectasia), venous duplex examination was normal apart from a small incompetent perforator vein within the right calf.

Lymphoscintigraphy confirmed impaired lymphatic drainage within both lower limbs. Only 3.1% of tracer reached the right inguinal lymph nodes at two hours, and 5.7% reached the left inguinal lymph nodes. Rapid uptake of tracer was seen within tortuous lymphatic tracts in both lower limbs on the initial 15 minute scans, similar to those seen in Patient II:3 and Patient II:1.

Targeted Capture and Massive Parallel Sequencing

Whole exome capture was performed using the SureSelect Target Enrichment System (Agilent). This was followed by sequencing on a HiSeq200 (Illumina) with 100bp paired end reads; summary statistics are provided in Online Table I. Sequence reads were aligned to the reference genome (hg19) using Novoalign (Novocraft Technologies SdnBhd). Duplicate reads, resulting from PCR clonality or optical duplicates, and reads mapping to multiple locations were excluded from downstream analysis. Depth and breadth of sequence coverage were calculated with custom scripts and the BedTools package.¹

Read Mapping and Variant Analysis

Single-nucleotide substitutions and small indel variants were identified (Online Table II) and quality filtered within the SamTools software package² and in-house software tools.³ Variants were annotated with respect to genes and transcripts with the Annovar tool.⁴ Variants were filtered for novelty by comparing them to dbSNP135 and 1000 Genomes SNP calls and to variants identified in 650 control exomes (primarily of European origin), which we sequenced and analysed by the method described above. Initial analysis of our PL exome variant profiles is performed by filtering for a list of genes known to be involved in lymphatic development and maintenance, and a heterozygous frameshift variant in *VEGFC* was identified.

Confirmation Sequencing

Subsequently, the rest of the family (n=11) was screened for this *VEGFC* variant using Sanger sequencing. Previously designed primers⁵ for *VEGFC* (NM_005429.2) were used: 4F 5'-aacatagcgtcctgcgtaca-3' and 4R 5'-aaaatacgcttcccactgaa-3' (T_A = 57°, 1.5mM Mg⁺⁺). PCR products were sequenced using BigDye Terminator v3.1 and an ABI3130xla Genetic Analyser. Sequencing traces were visually inspected in Finch TV v1.4 (Geospiza Inc, Seattle, WA, USA). The variant co-segregated with the disease status in the family. A further 7 heterozygous nonsense and indel variants were identified in the exome of the proband, none of which cosegregated with disease in the family (Online Table III).

Sequencing of all seven *VEGFC* coding exons and flanking intronic areas (primer sequences and PCR conditions are available upon request) in a small selection of patients with a similar phenotype (n=16 MD *VEGFR3* mutation negative cases) did not reveal any *VEGFC* mutations, deletions or copy number variants. Furthermore, we have not identified additional *VEGFC* mutations in any of our other PL exomes (n>50, mix of PL phenotypes including MD-like phenotype).

Cloning

The mutant *VEGFC*insTT variant (h*VEGFC*insTT) was generated by amplifying the coding sequence of full length wildtype human *VEGFC* (h*VEGFC*) in a pCS2 vector, according to the

Mutation in *VEGFC* Causes Primary Lymphedema

QuikChange Site-Directed Mutagenesis protocol (Stratagene) and using the primer pair 5'gaaattacagtgcTTctctctcaaggcccaaac3' and 5'ggtttggggccttgagagagagAAgactgtaatttc3'. An IRES site followed by tagRFP was introduced downstream of the hVEGFC and hVEGFCinsTT in pCS2. For expression of human VEGF-C in the zebrafish floor plate, the hVEGFC IRES tagRFP and hVEGFCinsTT were each cloned into a plasmid containing the sonic hedgehog promoter and a floor plate specific enhancer (Ar-B)⁶ flanked by MiniTol2 sites.⁷ Diagrams of the constructs are shown in Online Figure I.

Western blot analysis of transiently transfected 293T cells

293T cells were transfected with the pCS2 expression vector coding for hVEGFC or hVEGFCinsTT using X-treme gene 9 (Roche) according to manufacturers' protocol. Three days post transfection conditioned medium was collected and cells were lysed in RIPA/SDS buffer. Conditioned media and cell lysates were mixed with Laemmli buffer and analyzed by Western blotting using VEGFC specific antibodies binding to the N-terminus of the VEGF homology domain (VEGFC isoform 103 antibody, antibodies-online).

Zebra fish assay

All zebrafish strains were maintained in the Hubrecht Institute using standard husbandry conditions. Animal experiments were approved by the Animal Experimentation Committee of the Royal Netherlands Academy of Arts and Sciences (DEC). The transgenic reporter line *TG(flt4:yfp)*, marking blood and lymphatic endothelial cells, was generated from BAC DKEY-58G10, using standard methods⁸, and will be described in detail elsewhere.

Ectopic over-expression in the floorplate was driven by a *sonic hedgehog* promoter and a floorplate specific activator region⁶ and an estimate of the expression of hVEGFC was obtained and monitored by simultaneous expression of tagRFP. Plasmids encoding the hVEGFC or hVEGFCinsTT cDNA and the floorplate specific promoter and enhancer regions flanked by MiniTol2sites,⁷ were co-injected at 25 ng/ μ l together with tol2 transposase mRNA (25 ng/ μ l) into zebrafish eggs at the 1-2 cell stage. Embryos were selected at 2 dpf for comparable expression of tagRFP and imaged at 56 hpf on a Leica SPE confocal microscope. An estimate of the expression of VEGFC was obtained and monitored by simultaneous expression of tagRFP or mturquoise. Due to technical limitations, the expression of mturquoise could not be imaged on this confocal microscope. Thus, mturquoise was imaged separately using a Leica AF7000 microscope. For quantification of vessel sprouting, both the sum of the YFP+ (Yellow Fluorescent Protein positive) area of all z-planes and the number of vessel branch points per area (200 x 300 microns) were analyzed using ImageJ (NIH, Bethesda, Maryland, USA). Data sets were tested for normality (Shapiro-Wilk) and equal variance. P-values were determined by Student's t-test. Values are presented as means \pm standard error of mean values (SEM). * = P<0.05; ** = P<0.01; *** = P<0.001.

Online Figure I. Diagram of construct

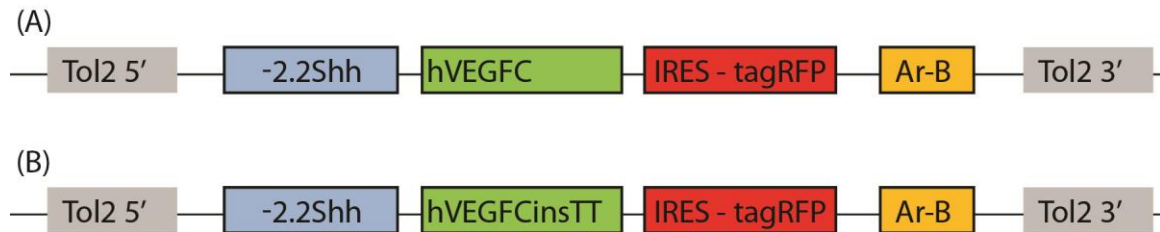
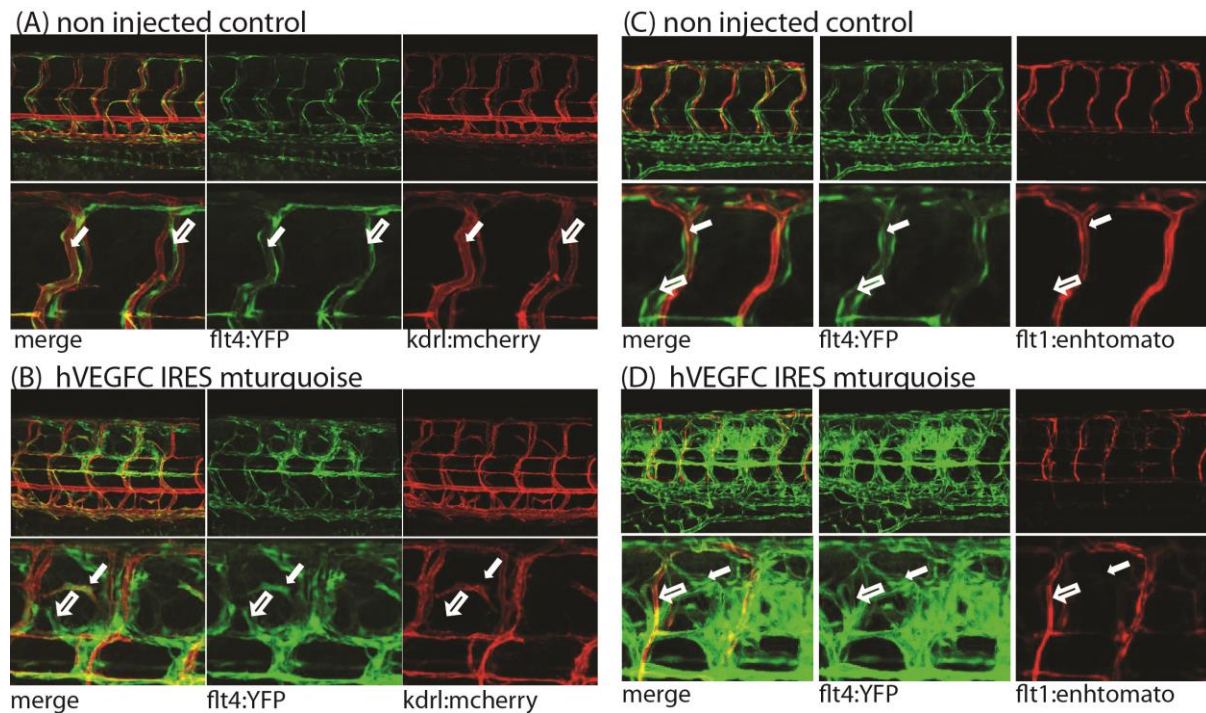


Diagram of constructs used for forced expression of either **(A)** hVEGFC or **(B)** hVEGFCinsTT together with tagRFP in the floorplate, consisting of a 5' and 3' Tol2 element, the -2.2Shh promoter region, the cDNA of human VEGFC wildtype or human VEGFC TTins, an IRES tagRFP cassette and the activating region Ar-B driving expression in the floorplate.

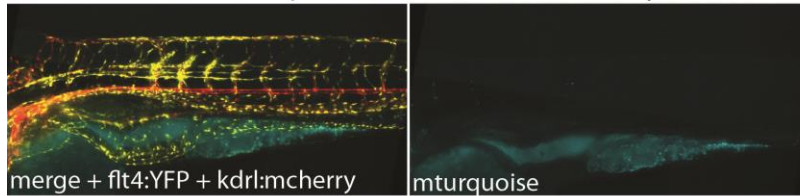
Online Figure II. hVEGFC promotes hypersprouting of venous and lymphatic vessels



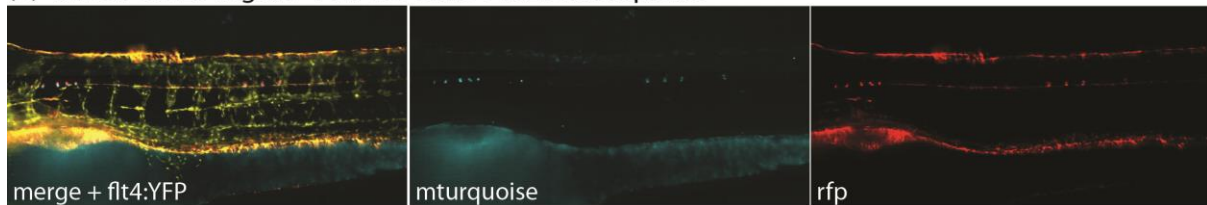
Analysis of hVEGFC overexpression in the floorplate using the transgenic lines TG(*flt4:YFP*), TG(*kdrl:mcherry*) and TG(*flt1:enhtomato*) at 5 dpf. *mturquoise* could not be imaged simultaneously with other fluorophores, thus we imaged this channel on another microscope (Online Figure III). **(A)** Non-injected control, the transgene *flt4:YFP* is expressed in venous and lymphatic vessels (white arrow) while the transgene *kdrl:mcherry* is expressed in blood endothelial cells (open arrow). **(B)** Forced expression of wildtype hVEGFC in the floorplate promotes hypersprouting of blood vessels (*flt4:YFP* and *kdrl:mcherry* positive, open arrow) and lymphatic vessels (only *flt4:YFP* positive, white arrow). **(C)** Non-injected control, the transgenes *flt4:YFP* and *flt1:enhtomato* allow discrimination between venous and lymphatic vessels (high *flt4:YFP*, low *flt1:enhtomato*, open arrow) and arterial vessels (low *flt4:YFP*, low *flt1:enhtomato*, white arrow). **(D)** Over-expression of hVEGFC in the floorplate resulted in excessive sprouting of venous and lymphatic vessels (high *flt4:YFP*, low *flt1:enhtomato*, open arrow), but not arterial vessels (low *flt4:YFP*, low *flt1:enhtomato*, white arrow).

Online Figure III. Expression of hVEGFC IRES mturquoise and hVEGFCinsTT IRES mturquoise

(A) hVEGFC IRES mturquoise in *flt4:YFP*; *kdr1:mcherry*



(B) hVEGFC IRES tagRFP + hVEGFCinsTT IRES mturquoise



Forced over-expression of hVEGFC IRES mturquoise or hVEGFCinsTT IRES mturquoise could not be imaged on the Leica SPE confocal microscope and was thus imaged on a Leica AF7000 microscope. **(A)** Forced over-expression of hVEGFC IRES mturquoise in *flt4:YFP*; *kdr1:mcherry* embryos. **(B)** Co-over-expression of hVEGFC IRES tagRFP and hVEGFCinsTT IRES mturquoise in *flt4:YFP* embryos. hVEGFC and hVEGFCinsTT are expressed in the same cells.

Online Table I. Summary statistics for exome sequencing

Sequenced Exomes	Number	Percentage
Uniquely mapped reads	92762461	
Uniquely mapped to target reads	61929112	66.76
Uniquely mapped to target +/-150bp reads	69799574	75.25
Accessible CCDS target bases	33323618	
Accessible CCDS target bases with coverage	32702247	98.14
Accessible CCDS target bases with coverage	30946670	92.87
Accessible CCDS target bases with coverage	29481297	88.47
Accessible CCDS target bases with coverage	27118137	81.38
Mean coverage		84.14

Total number of mapped reads and resulting coverage of the CCDS (Consensus Coding Sequence Project) exome in proband.

Online Table II. Summary statistics for exome sequencing - variant calling in proband

Variant type	Total	Known	Novel
All Variants	21465	21289	176
Heterozygous variants	13088	12925	163
Homozygous variants	8377	8364	13
Coding variants	18971	18819	152
Heterozygous coding variants	11557	11417	140
Homozygous coding variants	7414	7402	12
Splice site variants (10bp)	2494	2470	24
Heterozygous splice variants	1531	1508	23
Homozygous splice variants	963	962	1
Nonsynonymous SNVs	8821	8723	98
Heterozygous nonsynonymous SNVs	5419	5328	91
Homozygous nonsynonymous SNVs	3402	3395	7
Synonymous SNVs	9667	9625	42
Heterozygous synonymous SNVs	5877	5838	39
Homozygous synonymous SNVs	3790	3787	3
Stop loss SNVs	43	43	0
Heterozygous stop loss SNVs	23	23	0
Homozygous stop loss SNVs	20	20	0
Stop gain SNVs	93	90	3
Heterozygous stop gain SNVs	71	68	3
Homozygous stop gain SNVs	22	22	0
Deletions	155	150	5
Heterozygous deletions	84	80	4
Homozygous deletions	71	70	1
Insertions	167	163	4
Heterozygous insertions	66	63	3
Homozygous insertions	101	100	1
Frameshift deletions	70	66	4
Heterozygous frameshift deletions	39	36	3
Homozygous frameshift deletions	31	30	1
Frameshift insertions	95	93	2
Heterozygous frameshift insertions	27	25	2
Homozygous frameshift insertions	68	68	0
Transition:transversion ratio	2.97	2.97	2.62
Heterozygous transition:transversion	2.94	2.94	2.64
Homozygous transition:transversion	3.02	3.02	2.33

Numbers of variants of different classes identified by exome sequencing in the sequenced proband. SNV - single nucleotide variant.

Online Table III. Summary of sequencing results for all novel, heterozygous, nonsense and frameshift variants in the family

	VEGFC	C16orf59	CNTLN	OBSCN	MC1R	NCAPG	ANAPC1	OR2T12
	Frameshift	Nonsense	Nonsense	Frameshift	Frameshift	Frameshift	Nonsense	Frameshift
	c.571_572insTT	c.C742T	c.C3412T	c.21191delG	c.86_87insA	c.1266delA	c.C1115A	c.4_5del
	p.P191fs,	p.Q248X	R1138X	p.G7064fs	p.N29fs	p.K422fs	p.S372X	p.2_2del
II:4	Hetz	Hetz	Hetz	Hetz (del)	Hetz (del)	Hetz (del)	WT Homz	
I:2	Hetz	Hetz	Hetz	Hetz (del)	WT Homz	Hetz (del)		
I:1	WT Homz	WT Homz	WT Homz	WT Homz	Hetz (del)	WT Homz		
II:1	Hetz	WT Homz	WT Homz	Hetz (del)		Hetz (del)		
II:2	WT Homz	WT Homz	Hetz	WT Homz		WT Homz		
II:3	Hetz	Hetz	Hetz	WT Homz		WT Homz		
III:3	Hetz	Hetz	Hetz	WT Homz		Hetz (del)		
III:4	WT Homz	WT Homz	WT Homz	WT Homz		WT Homz		
III:2	Hetz	Hetz	WT Homz	WT Homz		WT Homz		
III:1	Hetz	Hetz	WT Homz	WT Homz		WT Homz		

In column 1, red: MD-like phenotype; green unaffected phenotype. In columns 2-8, red: carrier of heterozygous, mutant variant; green: homozygous wildtype. On Sanger sequencing, II:4 was homozygous wildtype for the ANAPC1, i.e. the observed variant was a false positive result from the exome. OR2T12 was extremely polymorphic and we were unable to design specific primers. However, this gene is an unlikely candidate. The frameshift variant identified in *VEGFC* is the only variant from the list of novel, heterozygous nonsense and frameshift variants in the exome of the proband that co-segregated with disease status in the family.

Supplement references

1. Quinlan AR, Hall IM. Bedtools: A flexible suite of utilities for comparing genomic features. *Bioinformatics*. 2010;26:841-842
2. Li H, Handsaker B, Wysoker A, Fennell T, Ruan J, Homer N, Marth G, Abecasis G, Durbin R, Genome Project Data P. The sequence alignment/map format and samtools. *Bioinformatics*. 2009;25:2078-2079
3. Simpson MA, Irving MD, Asilmaz E, Gray MJ, Dafou D, Elmslie FV, Mansour S, Holder SE, Brain CE, Burton BK, Kim KH, Pauli RM, Aftimos S, Stewart H, Kim CA, Holder-Espinasse M, Robertson SP, Drake WM, Trembath RC. Mutations in *notch2* cause hajdu-cheney syndrome, a disorder of severe and progressive bone loss. *Nature Genetics*. 2011;43:303-305
4. Wang K, Li MY, Hakonarson H. Annovar: Functional annotation of genetic variants from high-throughput sequencing data. *Nucleic Acids Research*. 2010;38:e164
5. Connell FC, Ostergaard P, Carver C, Brice G, Williams N, Mansour S, Mortimer PS, Jeffery S, Lymphoedema C. Analysis of the coding regions of *vegfr3* and *vegfc* in milroy disease and other primary lymphoedemas. *Human Genetics*. 2009;124:625-631
6. Ertzer R, Muller F, Hadzhiev Y, Rathnam S, Fischer N, Rastegar S, Strahle U. Cooperation of sonic hedgehog enhancers in midline expression. *Developmental Biology*. 2007;301:578-589
7. Balciunas D, Wangensteen KJ, Wilber A, Bell J, Geurts A, Sivasubbu S, Wang X, Hackett PB, Largaespada DA, McIvor RS, Ekker SC. Harnessing a high cargo-capacity transposon for genetic applications in vertebrates. *Plos Genetics*. 2006;2:1715-1724
8. Bussmann J, Schulte-Merker S. Rapid bac selection for *tol2*-mediated transgenesis in zebrafish. *Development*. 2011;138:4327-4332